AIAA JOURNAL
Vol. 44, No. 12, December 2006

Thermomechanical Stability of Imperfect Functionally Graded Plates Based on the Third-Order Theory

B. A. Samsam Shariat* and M. R. Eslami†
Amirkabir University of Technology, 15914 Tehran, Iran

DOI: 10.2514/1.19492

Mechanical and thermal buckling analysis of rectangular functionally graded plates with initial geometric imperfections is presented in this paper. It is assumed that the nonhomogeneous mechanical properties vary linearly through the thickness of the plate. The plate is assumed to be under three types of mechanical loadings, namely, uniaxial compression, biaxial compression, and biaxial compression and tension; and two types of thermal loadings, namely, the uniform temperature rise and nonlinear temperature gradient through the thickness. The equilibrium, stability, and compatibility equations are derived using the third-order shear deformation plate theory. Resulting equations are employed to obtain the closed-form solution for the critical buckling load for each loading case. The results are compared with the known data in the literature.

Nomenclature

a, b	=	plate length and width
$E(z)$, E_c, E_m	=	elasticity modulus of FGM, ceramic and metal
F_x, F_y	=	in-plane edge forces
$F_{x\mathrm{cr}}$	=	critical buckling force along the x-direction
h	=	plate thickness
$K(z)$, K_c, K_m	=	thermal conductivity of FGM, ceramic and metal
m, n	=	number of half waves in x- and y-directions
N_i, M_i, P_i, Q_i, R_i	=	stress resultants
R	=	load ratio
T	=	temperature
u, v, w	=	displacement components
w^*	=	initial imperfection
x, y, z	=	rectangular Cartesian coordinates
$\alpha(z)$, α_c, α_m	=	coefficient of thermal expansion of FGM, ceramic and metal
γ_{xy}, γ_{xz}, γ_{yz}	=	shear strains
ΔT_{cr}	=	critical buckling temperature change
ϵ_x, ϵ_y	=	normal strains
μ	=	imperfection coefficient
ν	=	Poisson's ratio
σ_x, σ_y	=	normal stresses
σ_{xy}, σ_{xz}, σ_{yz}	=	shear stresses

I. Introduction

MANY investigations are carried out on the subject of mechanical and thermal buckling of structures. Development of new materials, such as functionally graded materials (FGMs), have necessitated more research in this area. Functionally graded materials are new materials with heterogeneous/isotropic properties mainly designed to withstand high thermal stresses. Javaheri and Eslami reported mechanical and thermal buckling of rectangular functionally graded plates (FGPs) based on the classical plate theory (CPT) [1,2]. They used energy method and presented the closed-form solutions. They have also investigated thermal buckling of FGPs based on the higher-order displacement field [3]. The buckling loads are derived by solving the system of five stability equations. Motivated by Javaheri, Lanhe studied thermal buckling of moderately thick rectangular FGPs based on the first-order shear deformation theory (FSDT) [4]. He established a single stability equation and derived a closed-form solution for critical buckling temperature. Najafizadeh and Eslami studied the thermoelastic stability of circular functionally graded plates [5,6]. In the preceding references, perfect plates are considered.

The initial geometrical imperfections are inherent in many real engineering structures. Therefore, many researches are conducted on the stability analysis of imperfect structures. Brush and Almroth have presented the effect of initial imperfections on the critical buckling load of structures [7]. Elastic, plastic, and creep buckling of imperfect cylindrical shells under mechanical and thermal loads is studied by Eslami and Shariyat [8]. Mossavarali et al. studied the thermoelastic buckling of isotropic and orthotropic plates with initial imperfections [9,10]. Murphy and Ferreira have presented the thermal buckling analysis of clamped rectangular plates based on the energy consideration [11]. They determined the ratio of the critical temperature for a perfect flat plate to the one for an imperfect plate as a function of the initial imperfection size. The study includes analytical as well as experimental results. Eslami and Shahsiah reported the thermal buckling of imperfect circular cylindrical shells based on the Wan-Donnell and Koiter imperfection models [12]. The stability analysis of perfect FGPs has been presented by Shariat and Eslami based on the FSDT [13]. Shariat et al. reported the buckling of imperfect functionally graded plates under in-plane mechanical loading based on the classical plate theory [14]. Recently, the present authors have studied thermal buckling of such plates based on the classical and the first-order shear deformation theories [15,16].

The present article develops the thermal and mechanical buckling analysis of imperfect functionally graded plates on the basis of the third-order shear deformation theory (TSDT). The plate is graded linearly through the thickness direction. The boundary conditions are assumed to be simply supported. A double-sine function for the geometric imperfection along the x- and y-directions is considered. Using a suitable method, equilibrium equations are reduced from five to two equations. The corresponding stability equations are established. Using these equations, accompanied by the compatibility equation, yields the buckling loads in a closed-form

Received 15 August 2005; revision received 10 June 2006; accepted for publication 15 September 2006.

*Graduate student, Mechanical Engineering Department.
†Professor, Mechanical Engineering Department; eslami@aut.ac.ir (corresponding author). Associate Fellow AIAA.

solution for each loading case. The results are validated with the known data in the literature.

II. Fundamental Equations

Consider a rectangular functionally graded plate of length a, width b, and thickness h, referred to the rectangular Cartesian coordinates (x, y, z). We assume that the overall material properties of the plate vary linearly with respect to the thickness coordinate $z(-\frac{h}{2} \le z \le \frac{h}{2})$ as [2]

$$Pr(z) = Pr_m + Pr_{cm}\left(\frac{2z+h}{2h}\right) \qquad Pr_{cm} = Pr_c - Pr_m \tag{1}$$

where Pr denotes a material property of FGP with subscripts m and c referring to the metal and ceramic constituents, respectively. The variation of modulus of elasticity E, the coefficient of thermal expansion α, and the coefficient of heat conduction K of FGP across the thickness of the plate are assumed to be of the form given by Eq. (1). The materials are assumed to be isotropic. The Poisson's ratio ν is considered to be constant.

The third-order shear deformation theory, used in the present study, is based on the following displacement field [17]:

$$\begin{aligned} u(x,y,z) &= u_0 + zu_1 - \frac{4z^3}{3h^2}(u_1 + w_{0,x}) \\ v(x,y,z) &= v_0 + zv_1 - \frac{4z^3}{3h^2}(v_1 + w_{0,y}), \qquad w(x,y,z) = w_0 \end{aligned} \tag{2}$$

Here, u, v, and w are the total displacement components along the x-, y-, and z-directions, respectively, u_0, v_0, and w_0 are the middle plane displacements, and u_1 and v_1 are the rotations about the y- and x-axes, respectively. The parameters u_0, v_0, w_0, u_1, and v_1 are all functions of x and y variables. The general stain-displacement relations are [7]

$$\begin{aligned} \epsilon_x &= u_{,x} + \frac{1}{2}w_{,x}^2 \qquad \epsilon_y = v_{,y} + \frac{1}{2}w_{,y}^2 \\ \gamma_{xy} &= u_{,y} + v_{,x} + w_{,x}w_{,y} \qquad \gamma_{xz} = u_{,z} + w_{,x} \qquad \gamma_{yz} = v_{,z} + w_{,y} \end{aligned} \tag{3}$$

Substituting Eqs. (2) in Eqs. (3) gives the kinematic relations as [3]

$$\begin{aligned} \begin{pmatrix} \epsilon_x \\ \epsilon_y \\ \gamma_{xy} \end{pmatrix} &= \begin{pmatrix} \epsilon_x^0 \\ \epsilon_y^0 \\ \gamma_{xy}^0 \end{pmatrix} + z\begin{pmatrix} k_x^0 \\ k_y^0 \\ k_{xy}^0 \end{pmatrix} + z^3\begin{pmatrix} k_x^2 \\ k_y^2 \\ k_{xy}^2 \end{pmatrix} \\ \begin{pmatrix} \gamma_{xz} \\ \gamma_{yz} \end{pmatrix} &= \begin{pmatrix} \gamma_{xz}^0 \\ \gamma_{yz}^0 \end{pmatrix} + z^2\begin{pmatrix} k_{xz}^1 \\ k_{yz}^1 \end{pmatrix} \end{aligned} \tag{4}$$

where

$$\begin{aligned} \begin{pmatrix} \epsilon_x^0 \\ \epsilon_y^0 \\ \gamma_{xy}^0 \end{pmatrix} &= \begin{pmatrix} u_{0,x} + \frac{1}{2}w_{0,x}^2 \\ v_{0,y} + \frac{1}{2}w_{0,y}^2 \\ u_{0,y} + v_{0,x} + w_{0,x}w_{0,y} \end{pmatrix} \\ \begin{pmatrix} \gamma_{xz}^0 \\ \gamma_{yz}^0 \end{pmatrix} &= \begin{pmatrix} u_1 + w_{0,x} \\ v_1 + w_{0,y} \end{pmatrix} \\ \begin{pmatrix} k_x^0 \\ k_y^0 \\ k_{xy}^0 \end{pmatrix} &= \begin{pmatrix} u_{1,x} \\ v_{1,y} \\ u_{1,y} + v_{1,x} \end{pmatrix} \\ \begin{pmatrix} k_{xz}^1 \\ k_{yz}^1 \end{pmatrix} &= \begin{pmatrix} \frac{-4}{h^2}(u_1 + w_{0,x}) \\ \frac{-4}{h^2}(v_1 + w_{0,y}) \end{pmatrix} \\ \begin{pmatrix} k_x^2 \\ k_y^2 \\ k_{xy}^2 \end{pmatrix} &= \begin{pmatrix} \frac{-4}{3h^2}(u_{1,x} + w_{0,xx}) \\ \frac{-4}{3h^2}(v_{1,y} + w_{0,yy}) \\ \frac{-4}{3h^2}(u_{1,y} + v_{1,x} + 2w_{0,xy}) \end{pmatrix} \end{aligned} \tag{5}$$

The stress resultants N_i, M_i, P_i, Q_i, and R_i are expressed as [3]

$$\begin{aligned} (N_i, M_i, P_i) &= \int_{-h/2}^{h/2} \sigma_i(1, z, z^3)\,\mathrm{d}z \qquad i = x, y, xy \\ (Q_i, R_i) &= \int_{-h/2}^{h/2} \sigma_{iz}(1, z^2)\,\mathrm{d}z \qquad i = x, y \end{aligned} \tag{6}$$

Using the Hooke's law together with Eqs. (1), (4), and (6) gives the constitutive relations as [3]

$$\begin{aligned} (N_x, M_x, P_x) &= \frac{1}{1-\nu^2}[(E_1, E_2, E_4)(\epsilon_x^0 + \nu\epsilon_y^0) + (E_2, E_3, E_5)(k_x^0 + \nu k_y^0) + (E_4, E_5, E_7)(k_x^2 + \nu k_y^2) - (1+\nu)(\phi_1, \phi_2, \phi_4)] \\ (N_y, M_y, P_y) &= \frac{1}{1-\nu^2}[(E_1, E_2, E_4)(\epsilon_y^0 + \nu\epsilon_x^0) + (E_2, E_3, E_5)(k_y^0 + \nu k_x^0) + (E_4, E_5, E_7)(k_y^2 + \nu k_x^2) - (1+\nu)(\phi_1, \phi_2, \phi_4)] \\ (N_{xy}, M_{xy}, P_{xy}) &= \frac{1}{2(1+\nu)}[(E_1, E_2, E_4)\gamma_{xy}^0 + (E_2, E_3, E_5)k_{xy}^0 + (E_4, E_5, E_7)k_{xy}^2] \\ (Q_x, R_x) &= \frac{1}{2(1+\nu)}[(E_1, E_3)\gamma_{xz}^0 + (E_3, E_5)k_{xz}^1] \\ (Q_y, R_y) &= \frac{1}{2(1+\nu)}[(E_1, E_3)\gamma_{yz}^0 + (E_3, E_5)k_{yz}^1] \end{aligned} \tag{7}$$

where

$$\begin{aligned} E_1 &= E_m h + \frac{E_{cm}h}{2} \qquad E_2 = \frac{E_{cm}h^2}{12} \qquad E_3 = \frac{E_m h^3}{12} + \frac{E_{cm}h^3}{24} \\ E_4 &= \frac{E_{cm}h^4}{80} \qquad E_5 = \frac{E_m h^5}{80} + \frac{E_{cm}h^5}{160} \qquad E_6 = \frac{E_{cm}h^6}{448} \\ E_7 &= \frac{E_m h^7}{448} + \frac{E_{cm}h^7}{896} \\ (\phi_1, \phi_2, \phi_3, \phi_4) &= \int_{-h/2}^{h/2} (1, z, z^2, z^3)E(z)\alpha(z)\Delta T(x,y,z)\,\mathrm{d}z \end{aligned} \tag{8}$$

Also, the equilibrium equations of a perfect functionally graded plate based on the third-order shear deformation theory are [3]

$$\begin{aligned} &N_{x,x} + N_{xy,y} = 0 \qquad N_{xy,x} + N_{y,y} = 0 \\ &Q_{x,x} + Q_{y,y} - \frac{4}{h^2}(R_{x,x} + R_{y,y}) + \frac{4}{3h^2}(P_{x,xx} + 2P_{xy,xy} + P_{y,yy}) + N_x w_{0,xx} + 2N_{xy}w_{0,xy} + N_y w_{0,yy} = 0 \\ &M_{x,x} + M_{xy,y} - Q_x + \frac{4}{h^2}R_x - \frac{4}{3h^2}(P_{x,x} + P_{xy,y}) = 0 \\ &M_{xy,x} + M_{y,y} - Q_y + \frac{4}{h^2}R_y - \frac{4}{3h^2}(P_{xy,x} + P_{y,y}) = 0 \end{aligned} \tag{9}$$

Using Eqs. (5) and (7), and assuming that the temperature variation is either linear with respect to x- and y-directions, or constant, the equilibrium Eqs. (9) may be reduced to a set of two equations as

$$\begin{aligned} &D\nabla^2(u_{1,x} + v_{1,y}) - \frac{4}{3h^2}B\nabla^4 w_0 + N_x w_{0,xx} + 2N_{xy}w_{0,xy} + N_y w_{0,yy} = 0 \\ &\frac{4}{3h^2}\left[E\nabla^2(u_{1,x} + v_{1,y}) - \frac{4}{3h^2}C\nabla^4 w_0\right] + F(u_{1,x} + v_{1,y}) + F(w_{0,xx} + w_{0,yy}) + N_x w_{0,xx} + 2N_{xy}w_{0,xy} + N_y w_{0,yy} = 0 \end{aligned} \tag{10}$$

where

$$A=\frac{E_1E_3-E_2^2}{(1-\nu^2)E_1}\qquad B=\frac{E_1E_5-E_2E_4}{(1-\nu^2)E_1}\qquad C=\frac{E_1E_7-E_4^2}{(1-\nu^2)E_1}$$
$$D=A-\frac{4}{3h^2}B\qquad E=B-\frac{4}{3h^2}C$$
$$F=\frac{1}{2(1+\nu)}\left(E_1-\frac{8}{h^2}E_3+\frac{16}{h^4}E_5\right) \tag{11}$$

For a geometrically imperfect plate, let $w^*(x,y)$ denote a known small imperfection. This parameter represents a small deviation of the middle plane of the plate from a flat shape [18]. To consider the imperfections, the equilibrium Eqs. (10) are modified as

$$\begin{aligned}&D\nabla^2(u_{1,x}+v_{1,y})-\frac{4}{3h^2}B\nabla^4w_0+N_x(w_{0,xx}+w^*_{,xx})+2N_{xy}(w_{0,xy}\\&\quad+w^*_{,xy})+N_y(w_{0,yy}+w^*_{,yy})=0\\&\frac{4}{3h^2}\left[E\nabla^2(u_{1,x}+v_{1,y})-\frac{4}{3h^2}C\nabla^4w_0\right]+F(u_{1,x}+v_{1,y})+F(w_{0,xx}\\&\quad+w_{0,yy})+N_x(w_{0,xx}+w^*_{,xx})+2N_{xy}(w_{0,xy}+w^*_{,xy})+N_y(w_{0,yy}\\&\quad+w^*_{,yy})=0\end{aligned} \tag{12}$$

The stability equations of the plate may be derived by the adjacent equilibrium criterion [7]. Assume that the equilibrium state of the FGP under mechanical or thermal loads is defined in terms of the displacement components u^0, v^0, and w^0. The displacement components of a neighboring stable state differ by u^1, v^1, and w^1 with respect to the equilibrium position. Thus, the total displacements of a neighboring state are

$$u=u^0+u^1\qquad v=v^0+v^1\qquad w=w^0+w^1 \tag{13}$$

Similarly, the force resultants of a neighboring state may be related to the state of equilibrium as

$$N_x=N_x^0+N_x^1\qquad N_y=N_y^0+N_y^1\qquad N_{xy}=N_{xy}^0+N_{xy}^1 \tag{14}$$

where N_x^1, N_y^1, and N_{xy}^1 represent the linear parts of the force increments corresponding to u^1, v^1, and w^1. The stability equation may be obtained by substituting Eqs. (13) and (14) in Eqs. (12). We assume that the temperature variation is either linear with respect to x- and y-directions, or constant. Upon substitution, the terms in the resulting equations with superscript 0 satisfy the equilibrium condition and therefore drop out of the equations. Also, the nonlinear terms with superscript 1 are ignored because they are small compared to the linear terms. The remaining terms form the stability equations as

$$\begin{aligned}&D\nabla^2(u^1_{1,x}+v^1_{1,y})-\frac{4}{3h^2}B\nabla^4w_0^1+N_x^0w^1_{0,xx}+2N_{xy}^0w^1_{0,xy}+N_y^0w^1_{0,yy}\\&\quad+N_x^1(w^0_{0,xx}+w^*_{,xx})+2N_{xy}^1(w^0_{0,xy}+w^*_{,xy})+N_y^1(w^0_{0,yy}+w^*_{,yy})\\&\quad=0\\&\frac{4}{3h^2}\left[E\nabla^2(u^1_{1,x}+v^1_{1,y})-\frac{4}{3h^2}C\nabla^4w_0^1\right]+F(u^1_{1,x}+v^1_{1,y})+F(w^1_{0,xx}\\&\quad+w^1_{0,yy})+N_x^1(w^0_{0,xx}+w^*_{,xx})+2N_{xy}^1(w^0_{0,xy}+w^*_{,xy})+N_y^1(w^0_{0,yy}\\&\quad+w^*_{,yy})+N_x^0w^1_{0,xx}+2N_{xy}^0w^1_{0,xy}+N_y^0w^1_{0,yy}=0\end{aligned} \tag{15}$$

The superscript 1 refers to the state of stability and the superscript 0 refers to the state of equilibrium conditions. A stress function Φ may be defined as [10]

$$N_x^1=\Phi_{,yy}\qquad N_y^1=\Phi_{,xx}\qquad N_{xy}^1=-\Phi_{,xy} \tag{16}$$

Substitution of Eqs. (16) in Eq. (15) leads to

$$\begin{aligned}&D\nabla^2(u^1_{1,x}+v^1_{1,y})-\frac{4}{3h^2}B\nabla^4w_0^1+N_x^0w^1_{0,xx}+2N_{xy}^0w^1_{0,xy}+N_y^0w^1_{0,yy}\\&\quad+\Phi_{,yy}(w^0_{0,xx}+w^*_{,xx})-2\Phi_{,xy}(w^0_{0,xy}+w^*_{,xy})+\Phi_{,xx}(w^0_{0,yy}\\&\quad+w^*_{,yy})=0\\&\frac{4}{3h^2}\left[E\nabla^2(u^1_{1,x}+v^1_{1,y})-\frac{4}{3h^2}C\nabla^4w_0^1\right]+F(u^1_{1,x}+v^1_{1,y})+F(w^1_{0,xx}\\&\quad+w^1_{0,yy})+\Phi_{,yy}(w^0_{0,xx}+w^*_{,xx})-2\Phi_{,xy}(w^0_{0,xy}+w^*_{,xy})\\&\quad+\Phi_{,xx}(w^0_{0,yy}+w^*_{,yy})+N_x^0w^1_{0,xx}+2N_{xy}^0w^1_{0,xy}+N_y^0w^1_{0,yy}=0\end{aligned} \tag{17}$$

The compatibility equation of the imperfect FGPs may be written as [14,15]

$$\begin{aligned}&\frac{1}{E_1}\nabla^4\Phi-2w^1_{0,xy}(w^0_{0,xy}+w^*_{,xy})+w^1_{0,xx}(w^0_{0,yy}+w^*_{,yy})\\&\quad+w^1_{0,yy}(w^0_{0,xx}+w^*_{,xx})=0\end{aligned} \tag{18}$$

The stability Eqs. (17) and the compatibility Eq. (18) establish a set of three differential equations with three incremental variables w_0^1, Φ, and $(u^1_{1,x}+v^1_{1,y})$, which are used to obtain the buckling loads of imperfect FGPs. The terms with superscript 0 in these equations are substituted by the corresponding values obtained from the equilibrium Eqs. (12).

III. Mechanical Buckling Analysis

The simply supported plate is assumed to be under in-plane edge loads F_x and F_y, uniformly distributed along the edges $x=0$, a and $y=0$, b, respectively. The boundary conditions are defined as [1]

$$w=M_x=0\quad\text{on } x=0,a\qquad w=M_y=0\quad\text{on } y=0,b \tag{19}$$

The prebuckling resultant forces are [1]

$$N_x^0=-\frac{F_x}{b}\qquad N_y^0=-\frac{F_y}{a}\qquad N_{xy}^0=0 \tag{20}$$

The imperfections of the plate, considering the boundary conditions, are assumed as [7,18]

$$w^*=\mu h\sin\frac{m\pi x}{a}\sin\frac{n\pi y}{b}\qquad m,n=1,2,\ldots \tag{21}$$

where the coefficient μ varies between 0 and 1 and μh represents the

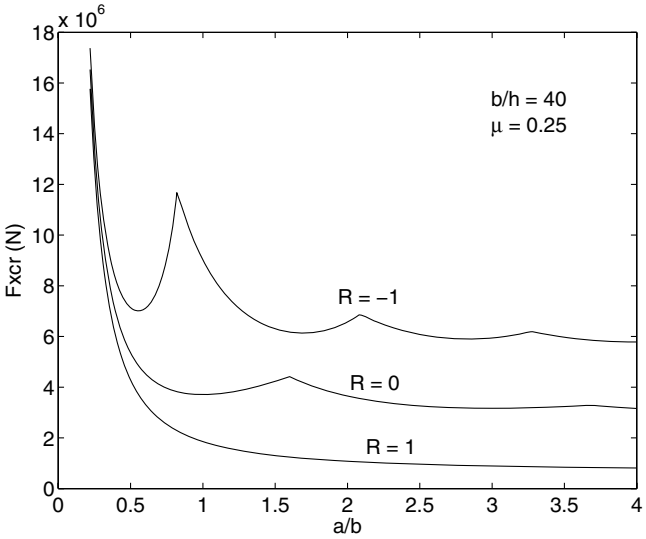

Fig. 1 Buckling load of imperfect FGPs under uniaxial compression ($R=0$), biaxial ($R=1$), and biaxial compression and tension ($R=-1$) vs aspect ratio, based on the third-order shear deformation theory.

imperfection size. Also, m and n are the number of half waves in x- and y-directions, respectively. To find the prebuckling deflection w_0^0, appeared in Eqs. (17) and (18), the following approximate solutions are assumed which satisfy both the equilibrium Eqs. (12) and the kinematical boundary conditions:

$$u_1^0 = u_{mn}^0 \cos\frac{m\pi x}{a}\sin\frac{n\pi y}{b} \qquad v_1^0 = v_{mn}^0 \sin\frac{m\pi x}{a}\cos\frac{n\pi y}{b} \qquad w_0^0 = w_{mn}^0 \sin\frac{m\pi x}{a}\sin\frac{n\pi y}{b} \qquad m,n = 1,2,\ldots \tag{22}$$

Substituting Eqs. (20–22) in the equilibrium Eqs. (12), w_0^0 is obtained as

$$w_0^0 = \frac{\mu h(F_x/b)G_{mn}^R[1 + (DG_{mn}/Q_{mn})]}{(DG_{mn}/Q_{mn})[FG_{mn} + (16C/9h^4)G_{mn}^2 - (F_x/b)G_{mn}^R] + (4B/3h^2)G_{mn}^2 - (F_x/b)G_{mn}^R}\sin\frac{m\pi x}{a}\sin\frac{n\pi y}{b} \tag{23}$$

where

$$G_{mn} = \left(\frac{m\pi}{a}\right)^2 + \left(\frac{n\pi}{b}\right)^2 \qquad G_{mn}^R = \left(\frac{m\pi}{a}\right)^2 + R\left(\frac{n\pi}{b}\right)^2 \qquad Q_{mn} = F - \frac{4}{3h^2}EG_{mn} \qquad R = \frac{F_y b}{F_x a} \tag{24}$$

Here, R is a nondimensional load parameter. The plate is under biaxial compression, when R is positive. It is subjected to the uniaxial compression along the x-axis, when $R = 0$. Negative values of R indicate compression and tension along the x- and y-directions, respectively. Substituting Eqs. (20), (21), and (23) in Eqs. (17) and (18) yields a set of three differential equations with three incremental variables w_0^1, Φ, and $(u_{1,x}^1 + v_{1,y}^1)$. To solve this set of equations, similar to the case of prebuckling analysis, we assume the following solutions [3]:

$$u_1^1 = u_{mn}^1 \cos\frac{m\pi x}{a}\sin\frac{n\pi y}{b} \qquad v_1^1 = v_{mn}^1 \sin\frac{m\pi x}{a}\cos\frac{n\pi y}{b} \qquad w_0^1 = w_{mn}^1 \sin\frac{m\pi x}{a}\sin\frac{n\pi y}{b} \qquad \Phi = \Phi_{mn}\sin\frac{m\pi x}{a}\sin\frac{n\pi y}{b}$$
$$m,n = 1,2,\ldots \tag{25}$$

Substituting the approximate solutions (25) into Eqs. (17) and (18) results in three nonzero residues R_1, R_2, and R_3. According to the Galerkin method, the residues are made orthogonal with respect to the assumed approximate solutions as [19]

$$\int_0^a\int_0^b R_1 \sin\frac{m\pi x}{a}\sin\frac{n\pi y}{b}dxdy = 0 \qquad \int_0^a\int_0^b R_2 \sin\frac{m\pi x}{a}\sin\frac{n\pi y}{b}\,\mathrm{d}x\,\mathrm{d}y = 0 \qquad \int_0^a\int_0^b R_3 \sin\frac{m\pi x}{a}\sin\frac{n\pi y}{b}\,\mathrm{d}x\,\mathrm{d}y = 0 \tag{26}$$

The determinant of the system of Eqs. (26) is set to zero, which results into the buckling load value

$$F_x = \frac{bG_{mn}^2\{(D/Q_{mn})[F + (16/9h^4)CG_{mn}] + (4/3h^2)B\} + b(I_{mn})^{1/3}}{G_{mn}^R[1 + (DG_{mn}/Q_{mn})]} \tag{27}$$

where

$$I_{mn} = \frac{1024E_1(Q_{mn} + DG_{mn})m^2n^2\pi^4\mu^2h^2G_{mn}^2}{9Q_{mn}a^4b^4}\left[\frac{D}{Q_{mn}}\left(F + \frac{16}{9h^4}CG_{mn}\right) + \frac{4}{3h^2}B\right]^2 \tag{28}$$

Note that these equations are derived for odd values of m and n. If either values of m or n are even, the system of Eqs. (26) results into the trivial solutions, which is unacceptable. The critical buckling force, $F_{x\mathrm{cr}}$, is the smallest value of F_x for the given values of the load ratio R and the aspect ratio a/b. Setting $\mu = 0$, the imperfection term I_{mn} vanishes and Eq. (27) is reduced to the buckling load of a perfect FGP.

IV. Thermal Buckling Analysis

A fixed-simply supported FGP is assumed to be under thermal loading. The edge conditions are [2,3,20]

$$u = v = w = M_x = 0 \quad \text{on } x = 0,a \qquad u = v = w = M_y = 0 \quad \text{on } y = 0,b \tag{29}$$

The prebuckling resultant forces are defined as [2,3,20]

$$N_x^0 = -\frac{\phi_1}{1-\nu} \qquad N_y^0 = -\frac{\phi_1}{1-\nu} \qquad N_{xy}^0 = 0 \tag{30}$$

where thermal parameter ϕ_1 is defined by the last of Eqs. (8). Substituting Eqs. (21), (22), and (30) in the equilibrium Eqs. (12), the prebuckling deflection w_0^0 due to the thermal load is obtained as

$$w_0^0 = \frac{\mu h[\phi_1/(1-\nu)][1 + (DG_{mn}/Q_{mn})]}{(D/Q_{mn})\{FG_{mn} + (16C/9h^4)G_{mn}^2 - [\phi_1/(1-\nu)]G_{mn}\} + (4B/3h^2)G_{mn} - [\phi_1/(1-\nu)]}\sin\frac{m\pi x}{a}\sin\frac{n\pi y}{b} \tag{31}$$

Similar to the solution procedure of the preceding section, substitution of Eqs. (21), (30), and (31) in Eqs. (17) and (18) yields a set of three differential equations with three incremental variables w_0^1, Φ, and $(u_{1,x}^1 + v_{1,y}^1)$. The approximate functions, given by Eqs. (25), are substituted into Eqs. (17) and (18), and the residues are made orthogonal similar to Eqs. (26). Finally, the unknown thermal parameter ϕ_1, which corresponds to the nontrivial solution of the system of Eqs. (26), is obtained as

$$\phi_1 = \frac{(1-\nu)G_{mn}\{(D/Q_{mn})[F + (16/9h^4)CG_{mn}] + (4/3h^2)B\} + (1-\nu)(I_{mn})^{1/3}}{1 + (DG_{mn}/Q_{mn})} \tag{32}$$

where

$$I_{mn} = \frac{1024E_1(Q_{mn} + DG_{mn})m^2n^2\pi^4\mu^2h^2}{9G_{mn}Q_{mn}a^4b^4}\left[\frac{D}{Q_{mn}}\left(F + \frac{16}{9h^4}CG_{mn}\right) + \frac{4}{3h^2}B\right]^2 \tag{33}$$

A. Uniform Temperature Rise

The plate initial temperature is assumed to be T_i. The temperature is uniformly raised to a final value T_f in which the plate under the assumed boundary conditions (29) buckles. The temperature change is $\Delta T = T_f - T_i$. Using Eqs. (1), (8), and (32), the buckling temperature change is obtained as

$$\Delta T = \frac{(1-\nu)G_{mn}\{(D/Q_{mn})[F + (16/9h^4)CG_{mn}] + (4/3h^2)B\} + (1-\nu)(I_{mn})^{1/3}}{L[1 + (DG_{mn}/Q_{mn})]} \tag{34}$$

where

$$L = E_m\alpha_m + \frac{E_m\alpha_{cm} + E_{cm}\alpha_m}{2} + \frac{E_{cm}\alpha_{cm}}{3} \tag{35}$$

The critical buckling temperature change, ΔT_{cr}, is the smallest value of ΔT for various values of m and n. This value is obtained when $m = 1$ and $n = 1$. Therefore,

$$\Delta T_{\text{cr}} = \frac{(1-\nu)G_{11}\{(D/Q_{11})[F + (16/9h^4)CG_{11}] + (4/3h^2)B\} + (1-\nu)(I_{11})^{1/3}}{L[1 + (DG_{11}/Q_{11})]} \tag{36}$$

where I_{11}, using Eq. (33), is defined as

$$I_{11} = \frac{1024E_1(Q_{11} + DG_{11})\pi^4\mu^2h^2}{9G_{11}Q_{11}a^4b^4}\left[\frac{D}{Q_{11}}\left(F + \frac{16}{9h^4}CG_{11}\right) + \frac{4}{3h^2}B\right]^2 \tag{37}$$

Setting $\mu = 0$, Eq. (36) is reduced to ΔT_{cr} for a perfect functionally graded plate.

B. Nonlinear Temperature Change Across the Thickness

The steady-state heat conduction equation and the boundary conditions are

$$\frac{\text{d}}{\text{d}z}\left(K(z)\frac{\text{d}T}{\text{d}z}\right) = 0 \qquad T = T_c \qquad z = \frac{h}{2}, \qquad T = T_m \qquad z = -\frac{h}{2} \tag{38}$$

where T_c and T_m are the temperatures of ceramic-rich and metal-rich surfaces, respectively. Using Eq. (1), the heat conduction equation becomes a function of z. The solution is obtained as

$$T(r) = T_m + \frac{\Delta T r\sum_{n=0}^{n=\infty}\{[-(rK_{cm}/K_m)]^n/(n+1)\}}{\sum_{n=0}^{n=\infty}\{[-(K_{cm}/K_m)]^n/(n+1)\}} \tag{39}$$

where $\Delta T = T_c - T_m$ and

$$r = \frac{2z + h}{2h} \tag{40}$$

Considering the temperature distribution expressed by Eq. (39), and using Eqs. (1), (8), and (32), the critical buckling temperature change across the thickness is defined as

$$\Delta T_{\text{cr}} = \frac{HG_{11}\{(D/Q_{11})[F + (16/9h^4)CG_{11}] + (4/3h^2)B\} + H(I_{11})^{1/3}}{1 + (DG_{11}/Q_{11})} \tag{41}$$

where I_{11} is defined by Eq. (37) and

$$H = \frac{(1-\nu)\sum_{n=0}^{n=\infty}\{[-(K_{cm}/K_m)]^n/(n+1)\}}{\sum_{n=0}^{n=\infty}\{[-(K_{cm}/K_m)]^n/(n+1)\}\{[E_m\alpha_m/(n+2)] + [(E_m\alpha_{cm} + E_{cm}\alpha_m)/(n+3)] + [E_{cm}\alpha_{cm}/(n+4)]\}} \tag{42}$$

V. Result and Discussion

The mechanical and thermal buckling loads of rectangular imperfect functionally graded plates, based on the third-order shear deformation theory, are obtained in closed-form solutions for the assumed types of loading and are represented by Eqs. (27), (36), and (41). These equations indicate that the buckling load values of an imperfect FGP is affected by the imperfection term I_{mn}, or I_{11} for the case of first buckling mode, which causes an increase in the buckling load values. Investigation of Eqs. (28) and (33) reveals that the imperfection term directly depends upon the imperfection coefficient μ. It is also affected by the material and geometrical properties of a functionally graded plate. The fact that the thermal buckling load of a plate is increased by the existence of geometrical imperfections is fully explained by Murphy and Ferreira [11]. The perfectly flat plate undergoes a symmetric pitchfork bifurcation at the buckling temperature. In contrast, the imperfect plate develops an asymmetric secondary state by means of a saddle-node bifurcation at the higher temperature [11]. This behavior also exists in the case of in-plane mechanical loading. The present study confirms this behavior for the functionally graded plates for both mechanical and thermal loads. As an example, we consider an imperfect ceramic-metal FGP that consists of aluminum and alumina with the following properties [1,2]:

$$E_m = 70 \text{ GPa} \qquad \alpha_m = 23e^{-6} \qquad K_m = 204 \text{ W/mK} \qquad E_c = 380 \text{ GPa} \qquad \alpha_c = 7.4e^{-6} \qquad K_c = 10.4 \text{ W/mK} \qquad \nu = 0.3 \tag{43}$$

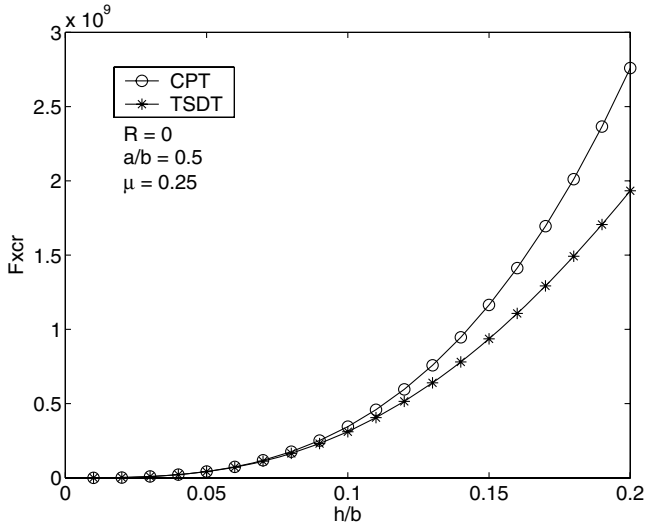

Fig. 2 Buckling load of imperfect FGPs under uniaxial compression vs relative thickness, based on the third-order shear deformation theory and the classical plate theory [14].

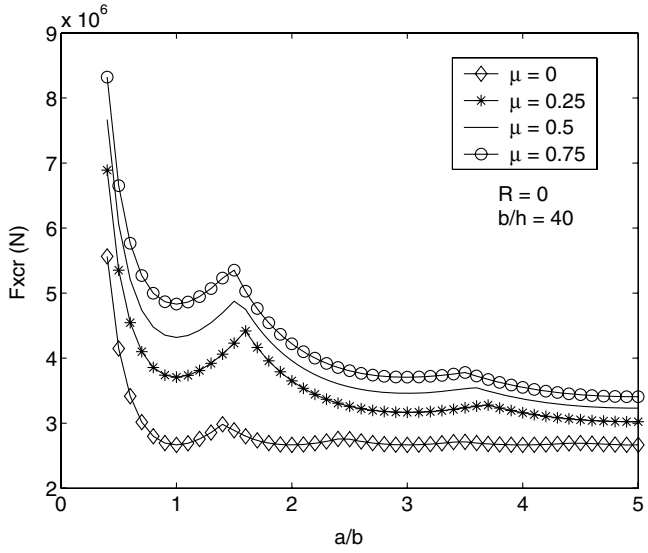

Fig. 3 Buckling load of FGPs under uniaxial compression vs aspect ratio and imperfection coefficient, based on the third-order shear deformation theory.

Because the transverse shear deformations are considered in this study, the assumed plate is not necessarily thin and may be a moderate thick plate. In the case of in-plane mechanical loading, for the given values of the load ratio R and the aspect ratio a/b, the values of m and n in Eq. (27) may be chosen by trial to give the smallest value of F_x, called F_{xcr}. These values are obtained by a suitable software. When $R = 1$, the critical buckling load for all

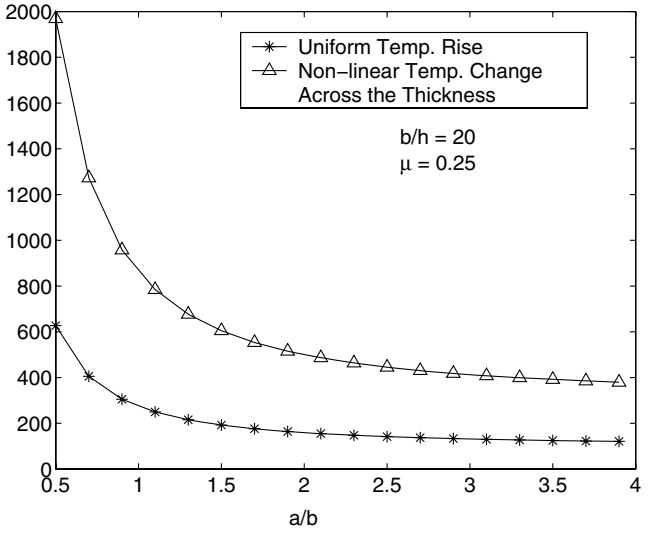

Fig. 4 Buckling temperature change of imperfect FGPs under uniform temperature rise and nonlinear temperature change across the thickness, vs aspect ratio, based on the third-order shear deformation theory.

aspect ratios corresponds to $m = 1$ and $n = 1$, which is the first mode of buckling. When $R = 0$ and -1, the critical buckling mode changes as the aspect ratio a/b is increased. In these cases $n = 1$, but the value of m depends upon the aspect ratio a/b. Figure 1 illustrates the variation of the critical buckling load F_{xcr} vs the aspect ratio a/b, under different types of in-plane mechanical loading based on the third-order shear deformation theory. The side-to-thickness ratio b/h and the imperfection coefficient μ are assumed to be 40 and 0.25, respectively. In general, the buckling load decreases by the increase of the aspect ratio a/b from 0.2 to 4. In the case of biaxial compression $R = 1$, the graph is smooth due to the unchanged buckling mode. As expected, the buckling load of the plate under uniaxial compression is greater than the one under biaxial compression and less than the one under biaxial compression and tension. Variation of F_{xcr} vs the relative thickness h/b is demonstrated in Fig. 2, using the third-order shear deformation theory (TSDT) and the classical plate theory (CPT) [14]. The imperfect plate is considered to be under uniaxial compression. It is observed that the buckling load is increased by the increase of the relative thickness h/b. The value of F_{xcr} obtained from the third-order shear deformation theory is lower than one from the classical plate theory. The difference between two theories is considerable for thicker plates ($h/b > 0.1$), but it may be neglected for thin plates. Figure 3 shows the effect of imperfection coefficient on the critical buckling load values. As seen, F_{xcr} increases by the increase of μ from 0 to 0.75. The increase of F_{xcr} from $\mu = 0$ to $\mu = 0.25$ is more considerable. Table 1 represents the comparison of the present work, for the case of a perfect plate ($\mu = 0$), with the classical plate theory, reported by Javaheri and Eslami [1], and the first-order shear deformation theory, reported by Shariat and Eslami [13]. The aspect ratio a/b is assumed to be 0.5. Figure 4 depicts the variation of ΔT_{cr}

Table 1 Buckling loads of a perfect FGP under in-plane loading vs side-to-thickness ratio, based on the classical [1], the first-order [13], and the third-order theories

R		$b/h = 10$	$b/h = 20$	$b/h = 40$	$b/h = 60$	$b/h = 80$	$b/h = 100$
0	CPT	267.48	33.435	4.1794	1.2383	0.5224	0.2675
	FSDT	243.41	32.628	4.1537	1.2349	0.5216	0.2672
	TSDT	239.15	32.472	4.1486	1.2343	0.5215	0.2672
1	CPT	213.99	26.748	3.3435	0.9907	0.4179	0.2140
	FSDT	194.73	26.103	3.3230	0.9880	0.4173	0.2138
	TSDT	191.32	25.978	3.3189	0.9879	0.4172	0.2137
−1	CPT	356.64	44.580	5.5725	1.6511	0.6966	0.3566
	FSDT	324.54	43.505	5.5383	1.6466	0.6955	0.3563
	TSDT	318.86	43.296	5.5315	1.6457	0.6953	0.3562

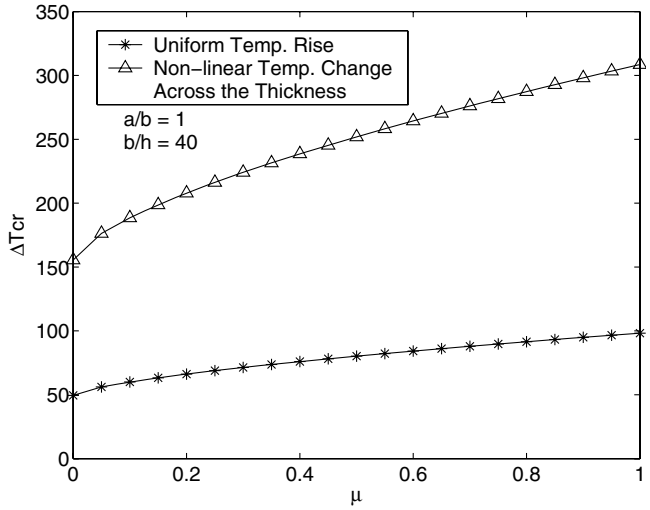

Fig. 5 Buckling temperature change of FGPs under uniform temperature rise and nonlinear temperature change across the thickness, vs imperfection coefficient based on the third-order shear deformation theory.

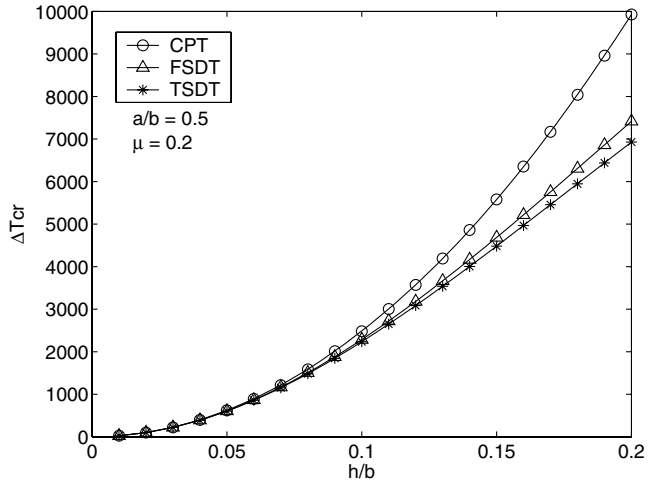

Fig. 6 Buckling temperature change of imperfect FGPs under uniform temperature rise vs relative thickness, based on the third-order, the first order [16], and the classical [15] plate theories.

vs the aspect ratio a/b, for the plate being subjected to two types of thermal loading. The side-to-thickness ratio b/h and the imperfection coefficient μ are considered to be 20 and 0.25, respectively. The plate buckles at the first mode for all aspect ratios. The plate under temperature gradient in the thickness direction buckles at higher temperature changes in comparison with uniform temperature rise. It is observed from Fig. 5 that the plate under temperature gradient across the thickness is more sensitive to initial imperfections than the same plate under uniform temperature rise. It is revealed that in both cases the thermal buckling loads increase by the increase of imperfection size. Figure 6 shows the comparison of the present work for the case of uniform temperature rise with the previous studies, based on the FSDT [16] and the CPT [15]. It is revealed that the transverse shear deformation has a large influence on the determination of ΔT_{cr}, especially for thick plates. Table 2 presents the results of buckling analysis of the plate under uniform temperature rise using various theories. It is seen that the results of the present work, based on the TSDT, are in good agreement with those reported by Lanhe [4] based on the FSDT, and Javaheri and Eslami [2] based on the CPT. It is inferred that for thick plates the differences between the theories are more considerable. To obtain acceptable results for thick functionally graded plates, it is necessary to consider the lateral shear deformations, using the shear deformation theories. Although the results of the TSDT and the FSDT are close to each other, it is recommended that one uses the TSDT for thick plates.

VI. Conclusions

In the present paper, equilibrium, stability, and compatibility equations of imperfect functionally graded plates are derived. Derivations are based on the third-order shear deformation theory and the linear composition of the constituent materials. The buckling analysis of such plates under different types of mechanical and thermal loads is presented. The followings are concluded:

1) In the case of mechanical loads, the critical buckling mode varies with respect to the load ratio R and/or the aspect ratio a/b. In case of thermal loads, however, the plate buckles at the first mode for all aspect ratios.

2) The classical plate theory overpredicts the critical buckling loads, especially for thick plates.

3) Buckling loads of FGPs increase by the increase of imperfection size.

4) For thick functionally graded plates, the third-order shear deformation theory provides more precise buckling load values.

5) Critical buckling loads of FGPs generally decrease with the increase of aspect ratio a/b, and increase with the increase of relative thickness h/b.

6) The plate under temperature variation across the plate thickness buckles at higher temperature changes in comparison with the uniform temperature rise.

References

[1] Javaheri, R., and Eslami, M. R., "Buckling of Functionally Graded Plates Under In-Plane Compressive Loading," *ZAMM*, Vol. 82, No. 4, 2002, pp. 277–283.

[2] Javaheri, R., and Eslami, M. R., "Thermal Buckling of Functionally Graded Plates," *AIAA Journal*, Vol. 40, No. 1, 2002, pp. 162–169.

[3] Javaheri, R., and Eslami, M. R., "Thermal Buckling of Functionally Graded Plates Based on Higher Order Theory," *Journal of Thermal Stresses*, Vol. 25, No. 7, 2002, pp. 603–625.

[4] Lanhe, W., "Thermal Buckling of a Simply Supported Moderately Thick Rectangular FGM Plate," *Composite Structures*, Vol. 64, No. 2, 2004, pp. 211–218.

[5] Najafizadeh, M. M., and Eslami, M. R., "Buckling Analysis of Circular Plates of Functionally Graded Materials Based on First Order Theory," *AIAA Journal*, Vol. 40, No. 7, 2002, pp. 1444–1450.

[6] Najafizadeh, M. M., and Eslami, M. R., "Thermoelastic Stability of Circular Plates Composed of Functionally Graded Materials Under

Table 2 Buckling temperature change of a perfect FGP under uniform temperature rise vs side-to-thickness and aspect ratios, based on the classical [2], the first-order [4], and the third-order theories

a/b		$b/h=10$	$b/h=20$	$b/h=40$	$b/h=60$	$b/h=80$	$b/h=100$
0.5	CPT	1985.9	496.49	124.12	55.17	31.03	19.85
	FSDT	1807.2	484.51	123.36	55.01	30.98	19.84
	TSDT	1775.6	482.18	123.21	54.98	30.97	19.84
0.25	CPT	6752.2	1688.1	422.01	187.56	105.50	67.52
	FSDT	5053.0	1557.1	413.33	185.83	104.95	67.30
	TSDT	4818.7	1533.6	411.63	185.48	104.84	67.25

Uniform Radial Compression," *International Journal of Mechanical Sciences*, Vol. 44, No. 12, 2002, pp. 2479–2493.

[7] Brush, D. O., and Almroth, B. O., *Buckling of Bars, Plates, and Shells*, McGraw–Hill, New York, 1975.

[8] Eslami, M. R., and Shariyat, M., "Elastic, Plastic, and Creep Buckling of Imperfect Cylinders Under Mechanical and Thermal Loading," *Journal of Pressure Vessel Technology*, Vol. 119, No. 1, 1997, pp. 27–36.

[9] Mossavarali, A., Peydaye Saheli, G., and Eslami, M. R., "Thermo-elastic Buckling of Isotropic and Orthotropic Plates with Imperfections," *Journal of Thermal Stresses*, Vol. 23, No. 9, 2000, pp. 853–872.

[10] Mossavarali, A., and Eslami, M. R., "Thermoelastic Buckling of Plates with Imperfections Based on Higher Order Displacement Field," *Journal of Thermal Stresses*, Vol. 25, No. 8, 2002, pp. 745–771.

[11] Murphy, K. D., and Ferreira, D., "Thermal Buckling of Rectangular Plates," *International Journal of Solids and Structures*, Vol. 38, Nos. 22–23, 2001, pp. 3979–3994.

[12] Eslami, M. R., and Shahsiah, R., "Thermal Buckling of Imperfect Cylindrical Shells.," *Journal of Thermal Stresses*, Vol. 24, No. 1, 2001, pp. 71–89.

[13] Shariat, B. A. S., and Eslami, M. R., "Buckling of Functionally Graded Plates Under In-Plane Compressive Loading Based on the First Order Plate Theory," *Proceeding of the 5th International Conference on Composite Science and Technology*, The School of Engineering, American Univ. of Sharjah, Sharjah, UAE, Feb. 2005, pp. 161–166.

[14] Shariat, B. A. S., Javaheri, R., and Eslami, M. R., "Buckling of Imperfect Functionally Graded Plates under In-Plane Compressive Loading," *Thin-Walled Structures*, Vol. 43, No. 7, 2005, pp. 1020–1036.

[15] Shariat, B. A. S., and Eslami, M. R., "Thermal Buckling of Imperfect Functionally Graded Plates," *International Journal of Solids and Structures*, Vol. 43, Nos. 14–15, 2006, pp. 4082–4096.

[16] Shariat, B. A. S., and Eslami, M. R., "Effect of Initial Imperfections on Thermal Buckling of Functionally Graded Plates," *Journal of Thermal Stresses*, Vol. 28, No. 12, 2005, pp. 1183–1198.

[17] Reddy, J. N., and Khdeir, A. A., "Buckling and Vibration of Laminated Composite Plates Using Various Plate Theories," *AIAA Journal*, Vol. 27, No. 12, 1988, pp. 1808–1817.

[18] Timoshenko, S. P., and Gere, J. M., *Theory of Elastic Stability*, McGraw–Hill, New York, 1961.

[19] Turvey, G., and Marshall, I., *Buckling and Postbuckling of Composite Plates*, Chapman–Hall, New York, 1995.

[20] Meyers, C. A., and Hyer, M. W., "Thermal Buckling and Postbuckling of Symmetrically Laminated Composite Plates," *Journal of Thermal Stresses*, Vol. 14, No. 6, 1991, pp. 519–540.

A. Roy
Associate Editor